DOI: 10.1002/ ((please add manuscript number))
Article type: Full Paper

High-performance Flexible Nanoporous Si-Carbon Nanotube Paper Anodes for Micro-battery applications

Erika Biserni[1,2], Alice Scarpellini[3], Andrea Li Bassi[~~2,3~~1,2], Paola Bruno[~~3~~1], Yun Zhou[4], Ming Xie[5,*]

1. Center for Nano Science and Technology @PoliMi, Istituto Italiano di Tecnologia, Via Pascoli 70/3, 20133 Milano, Italy
2. Department of Energy, Politecnico di Milano, Via Ponzio 34, 20133 Milano, Italy
3. Department of Nanochemistry, Istituto Italiano di Tecnologia, Via Morego 30, 16163 Genova, Italy
4. Chongqing Normal University, College of Chemistry, Chongqing, 401311, China
5. Wuhan ATMK Super EnerG Technologies Inc, Wuhan, P.R.China

Corresponding author: Ming Xie xmdxx1182@hotmail.com

Keywords: Nanoporous，fl~~i~~exible, Si-CNT paper anodes

Abstract

Nanoporous Si has been grown by Pulsed Laser Deposition on a free-standing carbon nanotube (CNT) paper sheet for micro-battery anodes. The Si deposition shows the conformal coverage on the CNT paper, and the Si-CNT paper anodes demonstrate high areal capacity of ~1000uAh/cm^2 at a current density of 54uA/cm^2, while, 69% of its initial capacity is preserved when the current density is increased by a factor 10. Excellent stability without capacity decay up to 1000 cycles at a current density of 1080uA/cm^2 is also demonstrated. After bending along the diameter of the circular paper disc many times, the Si-CNT paper anodes preserve the same morphology ~~and electrochemical performances~~, indicating that nanoporous Si-CNT paper anodes can find its application for flexible micro-batteries.

1. Introduction

With the rapid growth in the fields of microelectronics and wearable devices, the development of integrated flexible power sources that enable the continued device operation is of great importance. To meet these demanding applications, batteries with high energy and power density per unit area are urgently required [1-2]. In addition, wearable devices require that batteries should be highly flexible and have long cycling life. It would be also beneficial that the micro-battery fabrication process is compatible with state-of-the-art integrated circuit (IC) techniques in order to lower the costs.

Silicon alloys with lithium up to $Li_{15}Si_4$ [3-4] at room temperature, this resulting in a theoretical capacity almost 10 times larger (3579 mAh/g for $Li_{15}Si_4$) than that of graphite (372 mAh/g) [5], which is the standard commercial material for negative electrodes.

However, Si-based anodes need to overcome some major barriers for large-scale implementation in micro-batteries. First, they suffer from poor cycle life due to detrimental volume changes (i.e., theoretically up to 280% volume expansion[6]) of the host lattice upon alloying and de-alloying with Li. Extended fractures lead to a complete loss of electrical contact between active material and current collector and to pulverization. Second, the solid-electrolyte interphase ~~interface~~(SEI) layer in contact with common electrolytes is generally unstable and this detrimentally impacts on the capacity retention [7-8].

So far, silicon planar thin-film anodes for micro-batteries can only be realized within sub-μm thickness[9-13], leading to low areal capacities (mAh/cm^2). Therefore, it is important to develop Si thin film anodes with enhanced areal capacity, meanwhile offering a long and stable lifetime by managing mechanical instability due to volume changes. Secondly, the Cu current collector usually used for the anodes is very heavy and considered as "dead weight". It would be advantageous to eliminate the "dead weight" or replace it with some other lighter current collector, such as a carbon nanotube (CNT) paper which itself can also contribute to capacity. Fabrication of Si flexible micro-anodes by slurry coating with highly volatile organic solvents is incompatible with the state-of-the-art fabrication of microbatteries that usually require vacuum deposition.

Previously, we addressed these drawbacks by a two-layer architecture [14]. We fabricated novel nanocomposite Si-C anodes by depositing nanostructured porous amorphous Si films onto a Cu current collector by pulsed laser deposition (PLD) at room temperature, followed by chemical vapor deposition (CVD) of a thin carbon coating. The mesoporosity of the nanostructured Si films and its lack of crystallinity are expected to

reduce the detrimental effects of volume variations and to avoid mechanical stressing due to amorphization in the first cycle. The thin CVD-grown carbon layer is expected to promote the formation of a stable solid electrolyte interphase (SEI) layer and protect Si from direct contact with the electrolyte. In this work, we replace the Cu current collector with flexible CNT papers, and deposit Si film as thick as 3.5 μm by PLD but without the need for further CVD carbon coating. Eliminating the CVD step prevents high temperature processes and simplifies the whole process. These flexible free-standing Si-CNT paper anodes show a much higher capacity than that obtained in our previous work, and stable electrochemical performance up to 1000 cycles.

2. Experimental

2.1 CNT Paper Fabrication

Large-area CNT paper can be fabricated using a filtration method using a proprietary solvent developed by Wuhan ATMK Super EnerG Technologies Inc. Briefly, MWCNTs purchased from NanoTech Labs Inc. with a large aspect ratio of ~10^4, are dispersed by ultrasonic probe in the solvent without surfactants for 30 minutes. No organic binder is needed. The dispersion is then poured into a home-made vacuum filtration machine. The whole filtration process takes less than 15 seconds. Then the CNT paper with the filtration paper together is transferred into an oven at 100^{o}C for 4 hours until dried. Afterwards, CNT paper can be easily peeled off from the filtration paper. The size of CNT paper can be as large as 30cm by 30cm and its surface resistivity is as low as ~0.1Ω/□.

CNT paper prepared as here described has an areal weight of 21.7 g/m^2, which is much lower compared to the areal weight 806.4 g/m^2 of a Cu foil of the same thickness.

2.2 Si Film Deposition

Si films with the thickness of 3.5 μm were deposited on CNT substrates kept at room temperature by PLD in a mixture of Ar and H_2 as a background gas, with analogous procedure as described in our previous work [14]. The background gas pressure was set to 60Pa to reach a meaningful balance between introducing a considerable amount of pores in the film and preserving its mechanical stability. According to previous investigations, these deposition parameters allow to grow nanostructured films with hierarchical mesostructure where the cluster size is in the order of ~10nm.

Flexible CNT discs (1.3mm diameter, average thickness 90μm) were cut out from CNT paper and used as substrates. The thickness of Si film was determined from cross-sectional Scanning Electron Microscope images taken from a film deposited on a planar substrate under the same conditions. Samples for HRSEM, TEM and Raman analyses were prepared on purpose on a CNT substrate by depositing a 1μm-thick Si film under the same conditions.

2.3 SEM and TEM Characterizations

HRSEM images were taken with a JEOL JSM-7500F instrument, equipped with a cold field emission gun source and operating at 5 kV. TEM imaging and electron diffraction analyses were carried out with a Jeol JEM 1011 instrument, operated at 100 kV, equipped with a thermionic tungsten source. The sample, due to the weak and soft nature

of the CNTs disc, has been prepared by picking a small quantity of film with the tweezers and dispersing it in toluene, successively dropped it onto a holey carbon coated grid.

2.4 Raman Characterization

Raman spectra were acquired upon excitation by the second harmonic (532nm) of an air-cooled Nd:YAG laser. Laser power was kept below 0.4 mW (sample surface) while sampling Si films, in order to avoid laser-induced annealing effects. Spectra were recorded in the range 100-1800cm^{-1} in the Stokes region and were calibrated against the 520.5cm^{-1} line of an internal silicon wafer reference. The signal-to-noise ratio was enhanced by repeated acquisitions.

2.5 Electrochemical Characterization

Half-cells were assembled with Si-CNT papers with a diameter of 3/8" as working electrodes and Li metal foil as reference electrode. Si-CNT papers were bent 5 times along the diameter before cell assembling. The electrolyte was 1 M $LiPF_6$ dissolved in a 1:1 (volume ratio) mixture of ethylene carbonate (EC) and diethyl carbonate (DEC); the separator was a glass microfibre disc (Whatman GF/F), and the shell was a stainless steel CR2032 coin cell (VWR Inter.). Cells were then tested with an Arbin 2000 battery test station under constant current conditions, within the voltage range 1.5V - 5mV.

2.6 Bending test

In order to assess the bendability of Si-CNT anodes, a dedicated Si-CNT paper disc was bent repeatedly for 30 times along the diameter, so as to alternate traction-compression stresses on the film. To perform this bending test, the Si-CNT disc was bind to a paper sheet by taping two opposite points of one diameter; the paper sheet was then hold in

proximity of these two points and bent repeatedly by hands above and below the starting plane; bending amplitude was >45° above starting plane and >45° below. Bending frequency allowed to complete a whole bending cycle (above and below starting plane) in 1 second. With this procedure, the diameter perpendicular to the binding points sees the highest strain conditions.

3. Results and Discussion

Figure 1(a) and (b) (same scale) show the difference between the silicon-coated CNT paper and the uncoated sample. No silicon micrometer-size particles or agglomeration can be observed. The silicon coverage appears conformal along CNTs. The cross-section image in figure1(c) indicates that, due to the high presence of pores from the CNT paper, the silicon film has grown preferentially on each CNT as a nucleation site instead of forming a uniform layer like a film deposition onto a planar substrate. The Si film fabricated by PLD exhibits a hierarchically nanostructured morphology with mesoporosity, as shown in figure 1(d) and 2(a). Figure 2(a) evidences that the Si film covering the carbon nanotube has a hierarchically organized algae-like mesostructure. Bright field (BF) TEM images in figure 2(b) and (c) taken on the same sample confirm the hierarchical structure of the silicon film, with no trace of crystalline Si phases. Si film thickness assessed by SEM images on calibration samples returns the value of 3,5μm, thus accounting for a Si/C weight ratio estimate of 0,15.

From SEM and TEM images, it is clear that the Si film, while uniformly covering the CNT surface, keeps its nanogranular morphology and this promotes the formation of a

nanoscale/mesoscale porosity that consists of inter-cluster voids. In a previous work by some of the authors, the porosity of Si films grown with the same procedure was investigated by the Brunauer-Emmet-Teller method. The method analyses the adsorption/desorption isotherms of gases at low temperature to determine specific surface area of porous samples. Exploiting the BET theory, the calculated surface area of the film is 109 m^2/g. For more details on porosity characterization, the reader is addressed to [*please add DOI 10.1149/2.0531509jes].

In order to assess the bendability of Si-CNT anodes, a dedicated Si-CNT paper disc was bent repeatedly ~~for 30 times~~ along one diameter.~~, so as to alternate traction-compression stresses on the film.~~ From HRSEM images (figure 3(a-d)) taken ~~from~~ on the~~an~~ area ~~close to its diameter under~~ subjected to the highest strain conditions, the film looks almost intact with respect to the unstressed state and Si remains attached to CNT (figure 3(a, b)). Only in some spots, Si detaches from CNTs, as shown in figure 3(d). ~~All of the above images are obtained prior to cell assembling.~~

Raman spectra were acquired on dedicated samples made by depositing a 1µm-thick silicon film on a disc cut off a CNT paper (Figure 4). In the spectral range 50-600 cm^{-1} the features of amorphous Si are clearly visible, with the four characteristic Gaussian bands centred at 145, 330, 430 and 490 cm^{-1}, that are generally attributed to the transverse acoustic (TA), longitudinal acoustic (LA), longitudinal optic (LO) and transverse optic (TO) modes of amorphous silicon, respectively[15]. In the spectral range 1200-1800 cm^{-1} instead, the two D and G bands coming from the CNT foil are clearly defined (see reference spectrum taken on CNT foil), with D band (disordered carbon) being centred around 1350 cm^{-1} and G band (graphitic carbon) centred around 1590 cm^{-1}. As confirmed by Raman

spectroscopic analysis, Si film is fully amorphous and this is well consistent with BF-TEM observations and with previous analysis on Si film grown by PLD [*please add ref. DOI: 10.1007/s11051-014-2461-8].

In figure 5(a) the capacity of the Si-CNT anodes is presented under different areal current densities. The initial capacity of ~1500 μAh cm^{-2} is due to formation of the SEI layer, resulting in a 35% losses from the 2nd cycle. Si-CNT paper shows the highest capacity of ~1000 μAh cm^{-2} at 54 μA cm^{-2}. Some micro-battery anodes reported in literatures are summarized in Table1 for comparison with this work. At 540 μA cm^{-2}, 69% of its initial capacity is still preserved, indicating exceptional rate capability of Si-CNT paper anodes. Si-CNT paper anodes show excellent coulombic efficiency (>99%) when reaching stable condition. The mesoporous silicon on CNTs appears capable of tolerating volume change, as confirmed by the high coulombic efficiency during cycling.

Coulombic efficiency could be effectively increased by using additives to the electrolyte. In particular, the addition of Fluoroethylene carbonate and Vinylene carbonate has proven to be highly beneficial in the formation of a stable SEI and the reduction of irreversible losses [*please add DOI 10.1016/j.jpowsour.2012.08.066, DOI 10.1039/c4cp01948b and DOI 10.1039/c2cc31712e*]. In addition, initial coulombic efficiency can be further increased by a layer of alumina deposited by Atomic Layer Deposition [*please add ref. DOI 10.1021/ja205119g].

A silicon thin film with the same thickness of 3.5 μm was deposited onto a Cu current collector for comparison. Much lower capacities at various current densities and stability are observed in Figure 5(b). We believe CNT paper plays a very important role. First, CNT paper can contribute extra capacity as a current collector; secondly, CNT offers a pre-

formed porous substrate, leading to silicon deposition with increased mesoporosity, which can give enough space to tolerant volume expansion of silicon. Even under "stressful" conditions (current density of 1080 μA cm^{-2}), Si-CNT paper anodes behave in a very stable way, showing almost no capacity loss up to 1000 cycles (3% losses in the last 300 cycles), as shown in Figure 5(c). Although the area capacity drops dramatically when 1080 μA cm^{-2} is applied, for micro-batteries and wearable batteries power density is less critical for usage compared to the areal energy density and lifetime.

The charge/discharge curves of the first three cycles, measured between 5mV and 1.5V versus Li/Li^+ at a current density of 54μA/cm^2, are shown in Figure 5(d). The first lithiation curve shows a rapid drop of the potential with two plateaus: the first one, around 0.8V, can be related to the SEI formation, which concurs to irreversible capacity losses; the second one, around 0.3V is attributed to lithiation of amorphous silicon. In delithiation profiles, the smooth change in slope around 0.5V can be ascribed to delithiation of amorphous Li_xSi to give amorphous Si[16]. From the 2nd cycle, no plateau is observed during lithiation, which is the typical voltage profile of Li insertion/extraction in amorphous structure materials without phase transformation. These observations are consistent with other works [17-19]. We believe the ~~synergistic~~ synergetic effect of nanoporous amorphous structure and flexible CNT paper contribute to the excellent cycling performance of silicon with the thickness over 1um.

4. Conclusions

Nanoporous amorphous Si films have been produced by PLD in hierarchical mesoporous morphology and on a CNT paper current collector. The mesoporosity and the

crucial role of CNT substrate allowing for volume expansion of Si during charge/discharge have been exploited, resulting in very promising electrochemical performances. Capacity retention and rate capability are dramatically improved with respect to Si on Cu current collector, revealing the enhanced capacity of ~1000μAh/cm^2 at 54μA/cm^2 and a good stability with no decay for at least 1000 cycles at 1080μA/cm^2. Thanks to the combination of PLD and flexible CNT paper, it is possible to realize high-performance, flexible Si-CNT paper anodes for micro-batteries**.** The process-flow to obtain Si-CNT anodes, mainly based on PLD, can successfully minimize the required steps and reduce the involved temperatures. It allows to obtain free-standing anodes with minimized processing times/cost and to open the way to an up-scaled production of Si-based anodes for micro-batteries.

Acknowledgement

The work at Chongqing Normal University was supported by the Natural Science Foundation of China (No. 21301199), Chongqing Science and Technology Commission (cstc2014jcyjA50035), Chongqing Municipal Education Commission (KJ130601) and the Key Laboratory of Green Synthesis and Applications, College of Chemistry, Chongqing Normal University. This work at Wuhan ATMK Super EnerG Technologies Inc. is supported by the 3551 Recruitment Program of Global Experts by Wuhan East Lake Hi-Tech Development Zone, China. Erika Biserni would like to express her gratitude to Dr. Fabio Di Fonzo of the Centre for Nanoscience and Technology of IIT, Milan, for training and useful discussions on the pulsed laser deposition technique. Ming Xie and Erika Biserni contributed to this work equally.

References

[1] T. Jimbo, P. Kim and K. Suu, 2012 *2011 2nd International Conference on Advances in Energy Engineering (Icaee)* **14** 1574.

[2] A. Patil, V. Patil, D. W. Shin, J. W. Choi, D. S. Paik and S. J. Yoon, 2008 *Mater. Res. Bull.* **43** 1913.

[3] M. N. Obrovac and L. Christensen, 2004 *Electrochem. Solid St.* **7** A93.

[4] Y. H. Xu, G. P. Yin and P. J. Zuo, 2008 *Electrochim. Acta* **54** 341.

[5] Y. Kubota, M. C. S. Escano, H. Nakanishi and H. Kasai, 2007 *J. Appl. Phys.* **102**.

[6] M. N. Obrovac and L. J. Krause, 2007 *J. Electrochem. Soc.* **154** A103.

[7] D. E. Arreaga-Salas, A. K. Sra, K. Roodenko, Y. J. Chabal and C. L. Hinkle, 2012 *J. Phys. Chem. C* **116** 9072.

[8] M. Y. Nie, D. P. Abraham, Y. J. Chen, A. Bose and B. L. Lucht, 2013 *J. Phys. Chem. C* **117** 13403.

[9] M. D. Fleischauer, J. Li and M. J. Brett, 2009 *J. Electrochem. Soc.* **156** A33.

[10] H. J. Jung, M. Park, Y. G. Yoon, G. B. Kim and S. K. Joo, 2003 *J. Power Sources* **115** 346.

[11] S. Ohara, J. Suzuki, K. Sekine and T. Takamura, 2004 *J. Power Sources* **136** 303.

[12] M. N. He, Q. Sa, G. Liu and Y. Wang, 2013 *Acs Appl. Mater. Inter.* **5** 11152.

[13] H. J. Jung, M. Park, S. H. Han, H. Lim and S. K. Joo, 2003 *Solid State Commun.* **125** 387.

[14] E. Biserni, M. Xie, R. Brescia, A. Scarpellini, M. Hashempour, P. Movahed, S. M. George, M. Bestetti, A. Li Bassi and P. Bruno, 2015 *J. Power Sources* **274** 252.

[15] Z. Li, W. Li, Y. D. Jiang, H. H. Cai, Y. G. Gong and J. A. He, 2011 *J. Raman Spectrosc.* **42** 415.

[16] C. Pereira-Nabais, J. Swiatowska, A. Chagnes, A. Gohier, S. Zanna, A. Seyeux, P. Tran-Van, C. S. Cojocaru, M. Cassir and P. Marcus, 2014 *J. Phys. Chem. C* **118** 2919.

[17] E. Biserni, N. Garino, A. Li Bassi, P. Bruno and C. Gerbaldi, 2014 *ECS Transactions* **62** 107.

[18] S. H. Ng, J. Wang, D. Wexler, S. Y. Chew and H. K. Liu, 2007 *J. Phys. Chem. C* **111** 11131.

[19] W. R. Liu, J. H. Wang, H. C. Wu, D. T. Shieh, M. H. Yang and N. L. Wu, 2005 *J. Electrochem. Soc.* **152** A1719.

[20] W. Wei, G. Oltean, C. W. Tai, K. Edstrom, F. Bjorefors and L. Nyholm, 2013 *J. Mater. Chem. A* **1** 8160.

[21] J. H. Zhu, J. Jiang, Y. M. Feng, G. X. Meng, H. Ding and X. T. Huang, 2013 *Acs Appl. Mater. Inter.* **5** 2634.

[22] W. Wang, M. Tian, A. Abdulagatov, S. M. George, Y. C. Lee and R. G. Yang, 2012 *Nano Lett.* **12** 655.

[23] M. S. Park, G. X. Wang, H. K. Liu and S. X. Dou, 2006 *Electrochim. Acta* **51** 5246.

[24] J. B. Kim, H. Y. Lee, K. S. Lee, S. H. Lim and S. M. Lee, 2003 *Electrochemistry Commun.* **5** 544.

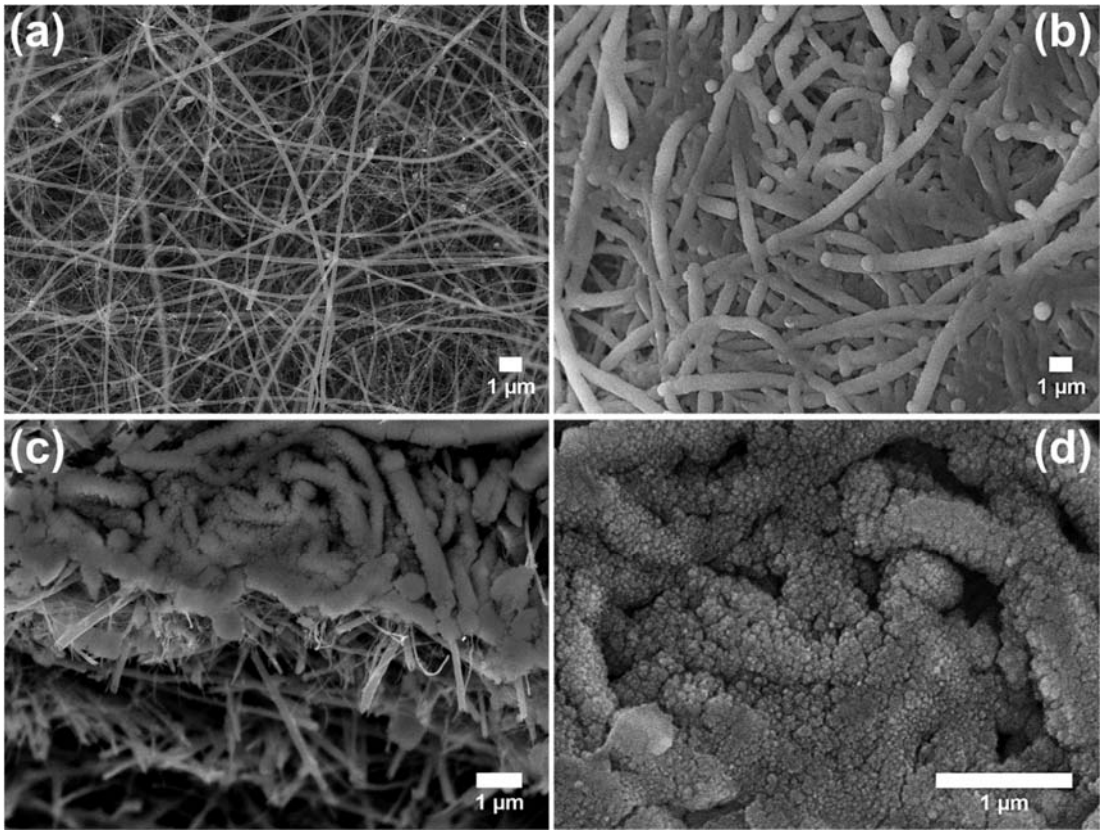

Figure 1. Top view SEM images of bare CNT paper (a) and Si-CNT (b). Cross-section images showing conformal covering of CNT by Si (c) and zoomed view of the Si morphology (d).

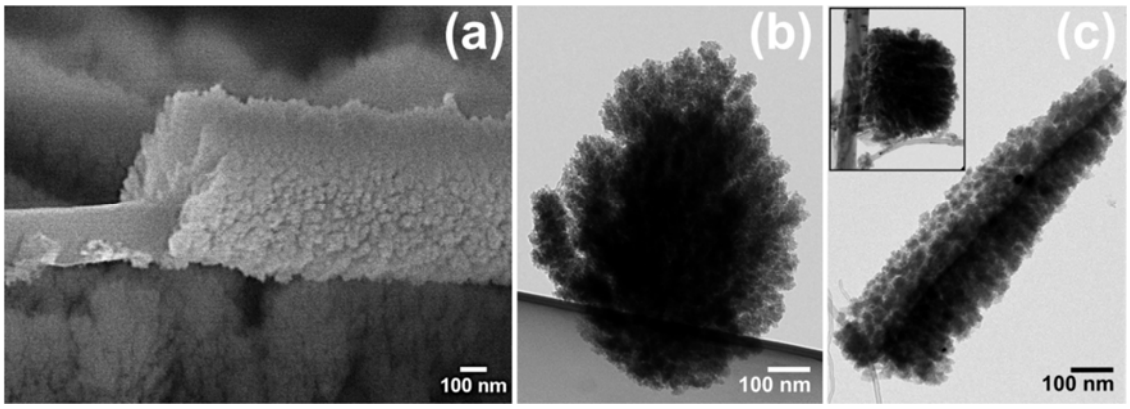

Figure 2. SEM (a) and TEM (b and c) images of Si covering a carbon nanotube.

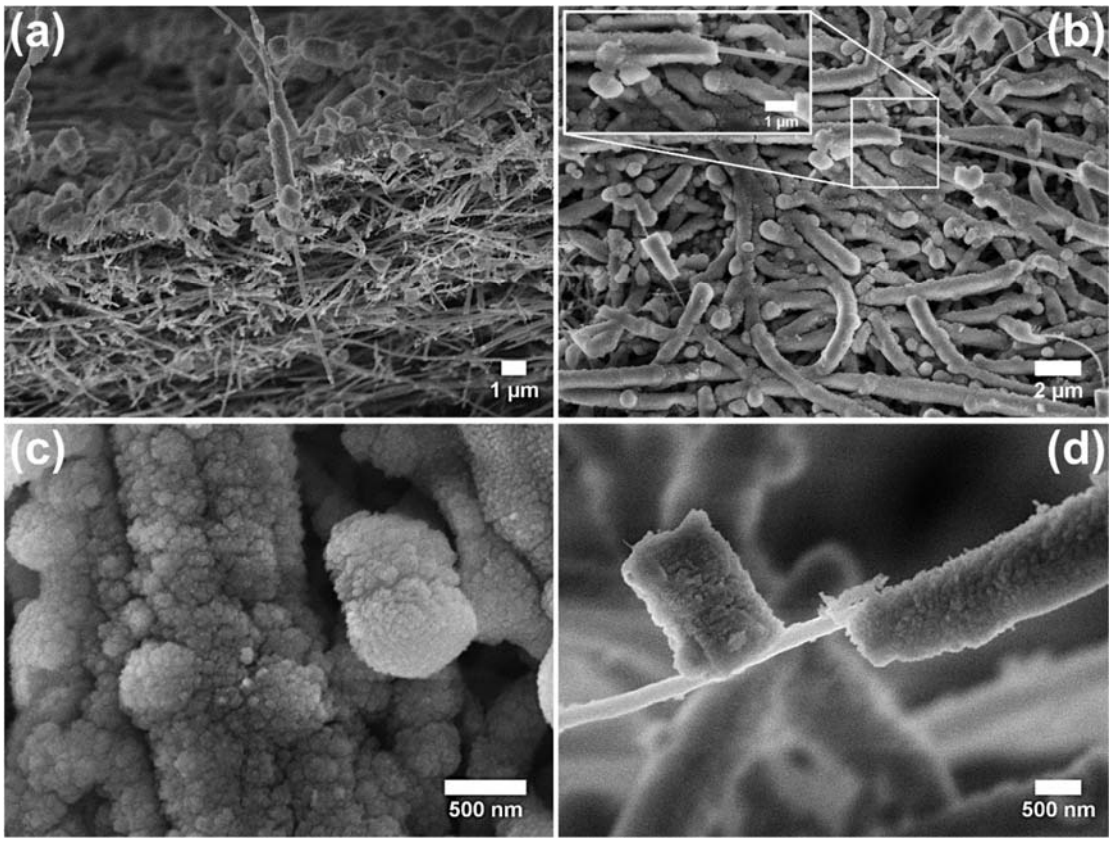

Figure 3. HRSEM images of Si-CNT after mechanical test. No visible damage is observed either in cross section (a) or plan view (b) The inset in (b) shows a zoomed view of the Si film covering a CNT. (c) Zoomed view of the silicon clustered film. (d) In some spots, silicon is detached from CNT.

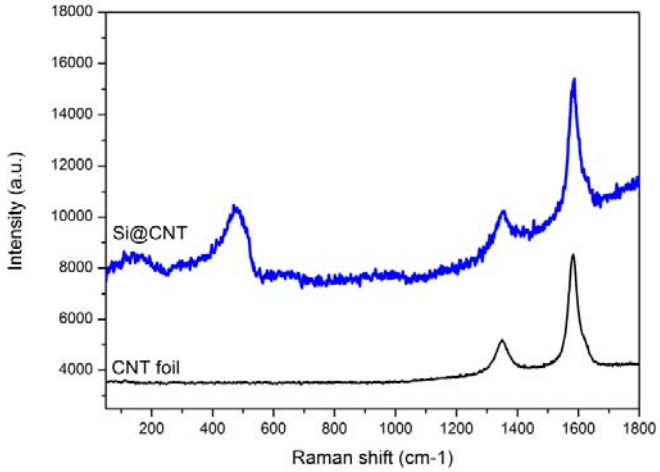

Figure 4. Raman spectrum of a Si-CNT sample with bare CNT foil spectrum as a comparison.

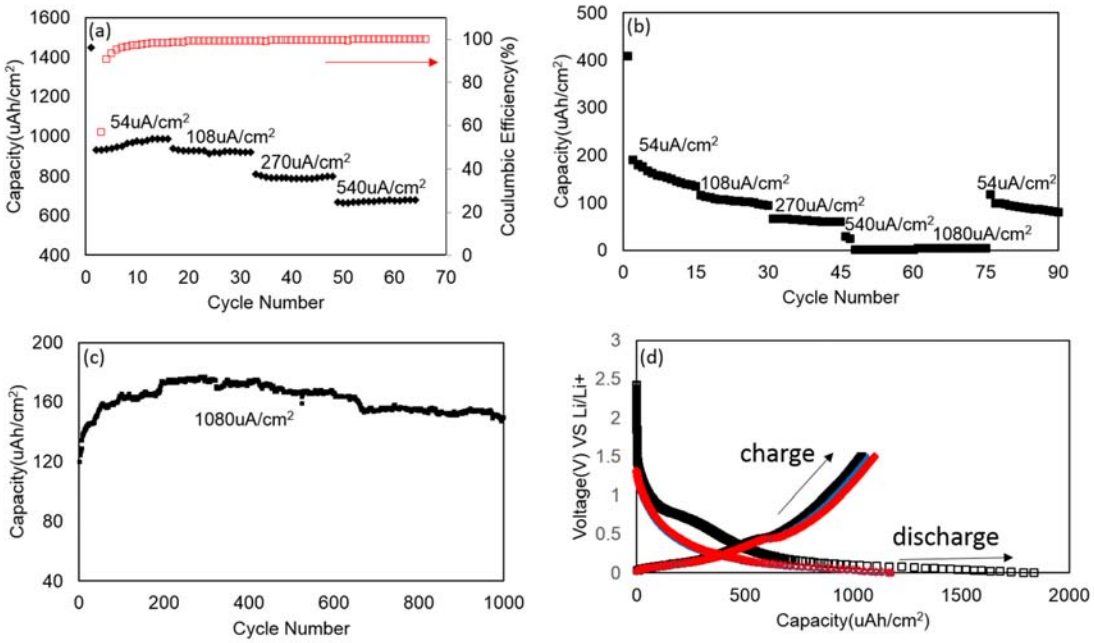

Figure 5. (a) Rate test and coulombic efficiency (b) Si film deposited onto Cu current collector under the same conditions (c) long life test, showing stable behavior up to 1000 cycles (d) Galvanostatic charge/discharge curves for the first three cycles.

363 Table1. Comparison of thin film battery anodes performance with this work

Materials	**Capacity(μAh cm^{-2})**	**Synthesis Technique**	**Reference**
Annealed TiO_2 nanotubes	460	two-step anodization followed by annealing	20
3D Ni/SnO_x/C nanostructured arrays	470	hydrothermal method followed by a calcination-reduction process	21
3D Ni/TiO_2 nanowire network	170	Electrodeposition followed by atomic layer deposition	22
3um Si on stainless steel	60	pulsed laser deposition	23
Fe/Si multi-layer thin film	130	electron-beam evaporation	24
CVD carbon coated nanoporous Si film on Cu	175	Pulsed laser deposition followed by chemical vapor deposition	14
3.5 μm nanoporous Si film on CNT paper	**1000**	**pulsed laser deposition**	**This work**

364

365